

## Electronic Supporting Information

### **Hierarchical NiO microflake films with high coloration efficiency, cyclic stability and low power consumption for applications in a complementary electrochromic device**

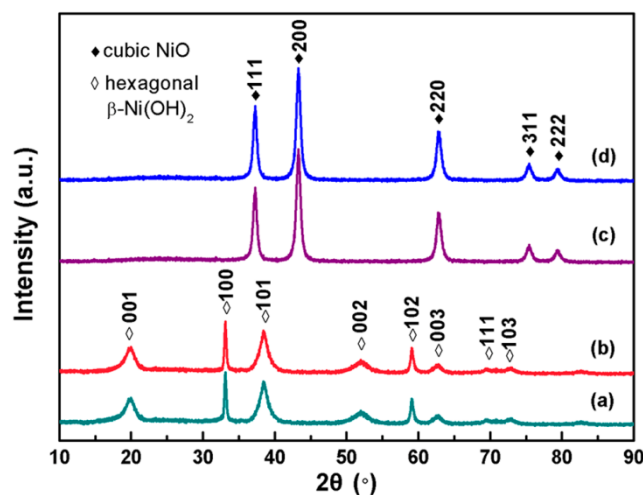
*Dongyun Ma,<sup>a</sup> Guoying Shi,<sup>c</sup> Hongzhi Wang,<sup>\*a</sup> Qinghong Zhang,<sup>b</sup> and Yaogang Li<sup>\*b</sup>*

*<sup>a</sup> State Key Laboratory for Modification of Chemical Fibers and Polymer Materials, College of Materials Science and Engineering, Donghua University, Shanghai 201620, P. R. China. Fax: +86-021-67792855; Tel: +86-021-67792881; E-mail: [wanghz@dhu.edu.cn](mailto:wanghz@dhu.edu.cn)*

*<sup>b</sup> Engineering Research Center of Advanced Glasses Manufacturing Technology, Ministry of Education, College of Materials Science and Engineering, Donghua University, Shanghai 201620, P. R. China. Fax: +86-021-67792855; Tel: +86-021-67792526; E-mail: [yaogang\\_li@dhu.edu.cn](mailto:yaogang_li@dhu.edu.cn)*

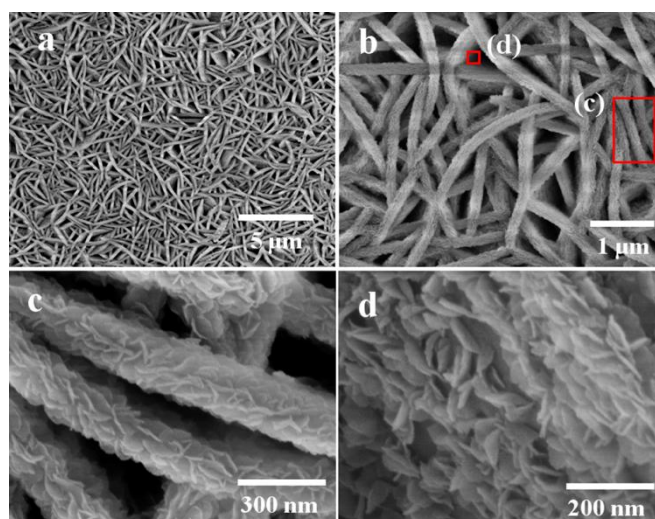
*<sup>c</sup> College of Chemistry, Chemical Engineering and Biotechnology, Donghua University, Shanghai 201620, China.*

Figure S1 shows the XRD patterns of the powders (collected from the bottom of the same autoclave) before and after annealing. From the XRD patterns, it was confirmed that all the diffraction peaks of the powders before and after annealing were indexed to the hexagonal  $\beta$ -Ni(OH)<sub>2</sub> structure (JCPDS no. 14-0117) and cubic NiO phase (JCPDS no. 04-0835), respectively, which agreed well with that of the as-deposited film.



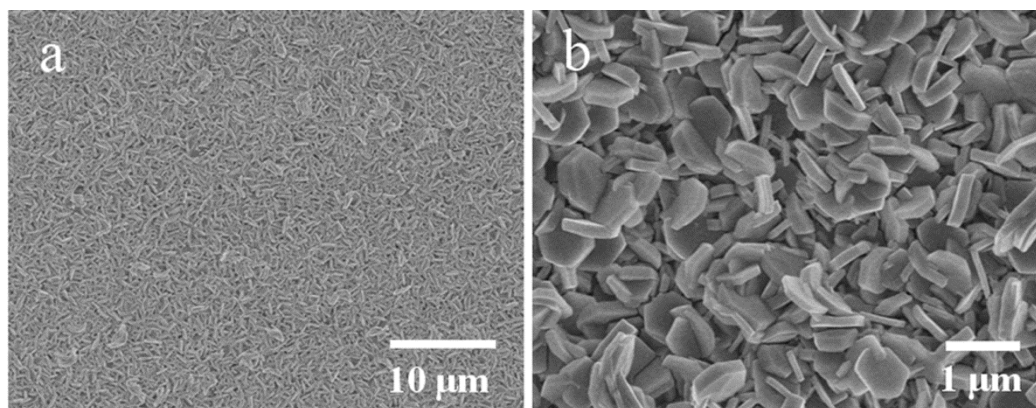
**Figure S1** XRD patterns for the (a, b) Ni(OH)<sub>2</sub> powders collected from the same reaction container as that for Ni(OH)<sub>2</sub> films growth and (c, d) NiO powders annealed at 400 °C for 2 h.

Figure S2 shows the FESEM images of the as-prepared hierarchical Ni(OH)<sub>2</sub> microflakes array film synthesized with addition of 0.36 mmol K<sub>2</sub>S<sub>2</sub>O<sub>8</sub> and 3 mL condensed aqueous ammonia. It can be seen that the film exhibited a porous architecture, which comprised of interconnected uniform microflakes that assembled from nanoleaves.



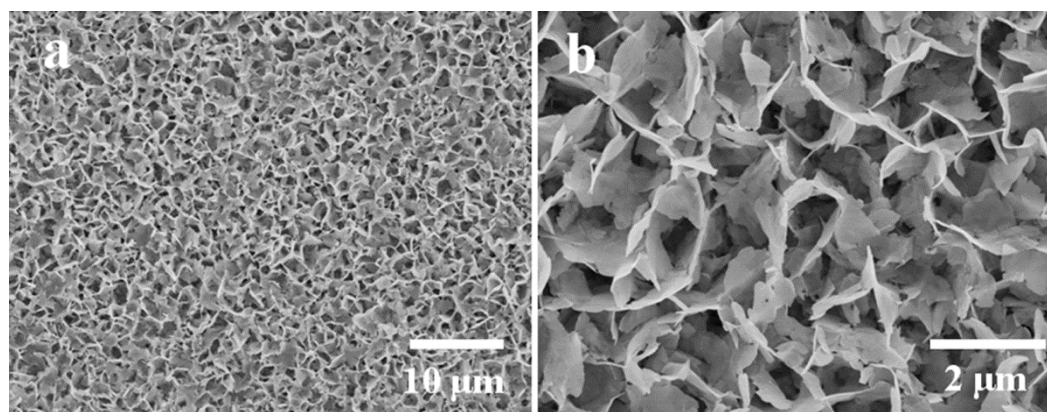
**Figure S2** FESEM images of Ni(OH)<sub>2</sub> films synthesized with addition of 3 mL condensed aqueous ammonia. (a) Low magnification and (b) higher magnification (c, d) the partial enlarged view corresponding to (c) and (d) marked in (b).

Figure S3 shows the FESEM images of the as-prepared hexagonal  $\text{Ni}(\text{OH})_2$  nanoplates film synthesized with addition of 0.36 mmol  $\text{K}_2\text{S}_2\text{O}_8$  and 6 mL condensed aqueous ammonia. As the amount of aqueous ammonia increased, the rate of homogeneous nucleation was accelerated, which may directly result in the thick nanoplate of  $\text{Ni}(\text{OH})_2$  during the high temperature; hence, the particle shape changed, giving hexagonal nanoplates instead of microflakes assembled from nanoleaves.



**Figure S3** FESEM images of  $\text{Ni}(\text{OH})_2$  films synthesized with addition of 6 mL condensed aqueous ammonia. (a) Low magnification and (b) higher magnification.

It is also worth noting that thin films of hierarchical NiO microflakes assembled from nanoleaves were obtained in the presence of  $K_2S_2O_8$ . Thus, the morphology of the as-synthesized NiO nanocrystals was influenced by the concentration of  $K_2S_2O_8$ . The nanoleaves can be assembled into microflakes under the assistance of negatively charged ions  $S_2O_8^{2-}$ . Figure S4 shows the FESEM images of the as-prepared  $Ni(OH)_2$  film synthesized in the absence of  $K_2S_2O_8$ . It can be seen that the nanoleaves can not be assembled into microflakes in the absence of  $K_2S_2O_8$  and the interconnected uniform nanosheets film was obtained due to Ostwald ripening.



**Figure S4** FESEM images of  $Ni(OH)_2$  films synthesized in the absence of  $K_2S_2O_8$ . (a) Low magnification and (b) higher magnification.